Chemical Physics Letters 539–540 (2012) 64–69

Contents lists available at SciVerse ScienceDirect

Chemical Physics Letters

journal homepage: www.elsevier.com/locate/cplett

Structure, stability and bonding in the $^1Au_{10}$ clusters

Jorge David [a,*], Doris Guerra [b], Albeiro Restrepo [b,*]

[a] Escuela de Ciencias y Humanidades, Departamento de Ciencias Básicas, Universidad Eafit AA 3300, Medellín, Colombia
[b] Grupo de Química–Física Teórica, Instituto de Química, Universidad de Antioquia, AA 1226 Medellín, Colombia

ARTICLE INFO

Article history:
Received 28 January 2012
In final form 19 April 2012
Available online 3 May 2012

ABSTRACT

A stochastic exploration of the quantum conformational space for the $^1Au_{10}$ system using a modified Metropolis acceptance test afforded 15 stable configurations in the MP2/SDDALL potential energy surface. The global minimum is predicted to be a 3D structure with D_{2d} symmetry. Topological analyses of the electron densities suggest that bonding appears to be of intermediate character, with substantial contributions from both covalent and closed shell interactions and that there is a direct correlation between the topological complexity of the electron density and cluster stability. Evidence regarding the nature of the interactions is gathered from many sources, including the total number of delocalized electrons (*nde*), a novel covalency index. Localization indices and condensed Fukui functions predict higher electron populations on peripheral, lowly coordinated atoms.

1. Introduction

The properties of gold clusters and nanoparticles are size and shape dependent. Among several important known examples of such dependencies, we cite considerably enhanced chemical and catalytic activity when compared to the bulk materials [1], improved roles in electronic [2] and optical [3] devices, etc. These, and other observations, have led to a growing number of scientific reports exploring the relationship between cluster morphology and properties [4–9].

The amount of experimental and theoretical work needed for complete structural characterization of potential energy surfaces (PES) as complex as that of $^1Au_{10}$ renders that aspiration impractical, nonetheless, a wealth of knowledge has accumulated in the literature for this particular system. One sensitive topic, for which an agreement has not been reached, is the structure and properties of the global minimum, which seems to depend on the level of theory used to calculate the PES. A well known observation, pointed out by Bonačić–Koutecký and coworkers [10] is the conflicting results afforded by DFT methods when compared to MP2 methodologies in the treatment of gold clusters, as a particular example, DFT methods predict planar geometries for Au_7^+ while MP2 methods favor 3D structures.

We discuss the recent literature (in chronological order, not intended as a review) dealing with the controversial issue of the global minimum for Au_{10} clusters. Wang and coworkers [11] using a combined DFT/genetic algorithms approach found the global minimum to be a C_{2v} 3D structure in agreement with previous reports by Häkkinen and Landman [12]. They also found that the transition from 2D → 3D structural preferences occurs at $n = 7$. Later, Walker [13] using several combinations of functionals and basis sets, found one 2D and one 3D structure 0.02 eV apart from each other. Sankaran and Viswanathan [14] also found a 3D structure to be the global minimum at the B3LYP/LANL2DZ level. A later study by Dong and Springborg [15] using a parameterized tight–binding density functional method combined with Genetic Algorithms reported a planar structure to be the global minimum. Planar preferences were also independently reported by Assadollahzadeh and Schwerdtfeger [16]. DFT, MP2, CCSD and CCSD(T) calculations led Choi and coworkers [17] to postulate a 2D global minimum; the same paper stresses the difficulties pointed out above in reconciling MP2 and DFT calculations in gold clusters. Kuang, Wang and Liu reported a planar structure as the global minimum using pure DFT methods and all electron relativistic scalar calculations at the DFT level [18–21]. A planar global minimum has been also predicted by Rincón and coworkers using a perturbatively corrected tight–binding method [22]. Needless to say, the several conflicting reports regarding the structure and properties of the global minimum and the relative energies of local minima in the $^1Au_{10}$ PES is an undesirable state of affairs.

In this work, we undertake a stochastic exploration of the $^1Au_{10}$ PES, followed by MP2/SDDALL characterization of all predicted stationary points, aiming at an exhaustive description of the conformational space. We present a topological analysis of the electron densities in order to gain insight into the intricate bonding that keeps the clusters as discrete units.

2. Computational details

The $^1Au_{10}$ PES was explored using the atomic cluster capabilities of the ASCEC program [23] which contains an adapted

* Corresponding authors.
E-mail addresses: jdavidca@eafit.edu.co (J. David), albeiro@mateticas.udea.edu.co (A. Restrepo).

0009-2614/$ - see front matter © 2012 Elsevier B.V. All rights reserved.
http://dx.doi.org/10.1016/j.cplett.2012.04.030

version of the Simulated Annealing optimization procedure. In the ASCEC algorithm [24,25], randomly generated structures resulting in negative energy changes ($\Delta E < 0$) are always accepted, while structures leading to positive energy changes ($\Delta E > 0$) are accepted if $\Phi(\Delta E) < P(\Delta E)$, where $P(\Delta E) = \exp(-\Delta E/k_B T)$ is the temperature dependent Boltzmann probability distribution function and $\Phi(\Delta E) = |\Delta E/E_j|$, j being the structure under evaluation (ΔE is calculated with respect to the structure that generated E_j). This acceptance criterion is more suitable in this line of problems than the classical Metropolis test of comparing $P(\Delta E)$ to a random number in the $[0, 1]$ interval, when potentially good structures can be randomly rejected. Specific details of the ASCEC method can be found elsewhere [24,25]. The ASCEC algorithm was used to generate candidate structures after random walks of the $^1Au_{10}$ PM6 [26] PES. The MP2/SDDALL model chemistry was used to optimize all local minima found in this work. The Stuttgart potentials used in this work include up to g orbitals for Au atoms [27,28]. Analytical harmonic vibrational frequencies at the same level were used to characterize all stationary points as true minima (no negative eigenvalues of the Hessian matrix). Binding energies (BE) at the same level were calculated by subtracting the energy of the cluster from the energy of the constituting atoms, in this way, larger positive numbers correspond to larger stabilization energies. All optimization, frequency, and energy calculations were carried out using the Gaussian 09 [29] suite of programs. Topological analyses of the electron densities were carried out along the lines implemented in the AIMQB program within the AIMStudio suite [30].

3. Results and discussion

3.1. ASCEC conditions

We used the big bang approach to construct the initial geometries for all ASCEC runs, namely, the ten Au atoms were placed at

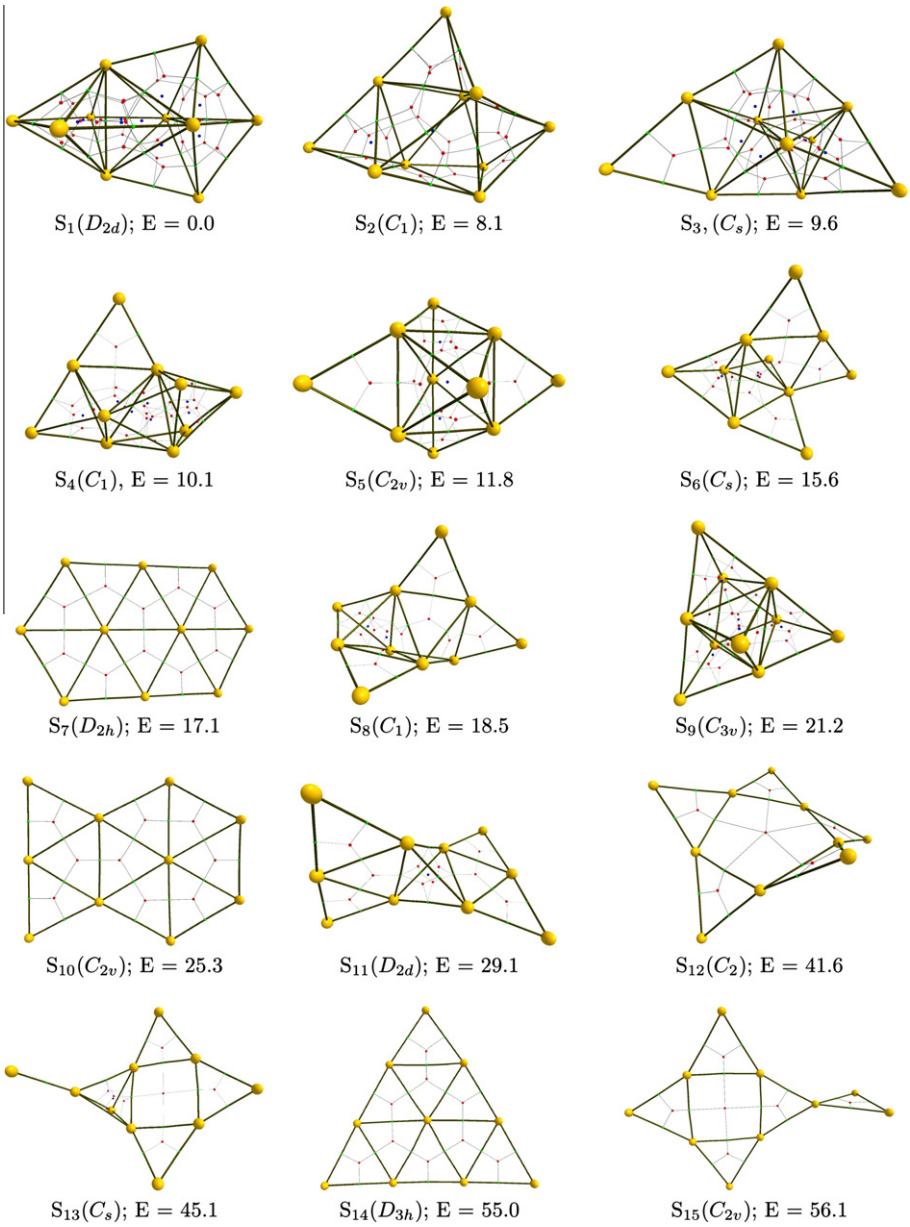

Figure 1. Molecular graphs for the local minima at the MP2/SDDALL level of theory for the $^1Au_{10}$ potential energy surface. Notation and relative energies in kcal/mol with respect to S_1 are included. Lines joining atoms are drawn to help visualization of the geometrical motifs. Green, red and blue dots correspond to bond, ring and cage critical points respectively. (For interpretation of the references to color in this figure legend, the reader is referred to the web version of this article.)

the same position, allowing them to evolve under the annealing conditions. The system was placed at the center of a cubic box of 9 Å of length; the PM6 parameterized Hamiltonian was used to calculate the energy of a Markovian chain of randomly generated configurations; we used a geometrical quenching route with initial temperature of 500 K, a constant temperature decrease of 5% and 100 total temperatures. The annealing was run twice under the same conditions.

3.2. Geometries and energies

$^1Au_{10}$ equilibrium geometries were produced following the procedure outlined above. All geometry optimizations were carried out with no imposition of symmetry constraints as the structures coming from ASCEC are randomly generated and belong to the C_1 point group; however, some of the located stationary points are very close to having higher effective symmetries.

The 15 equilibrium structures located on the MP2/SDDALL potential energy surface are depicted in Figure 1. The structures were named $S_1, S_2, \cdots, S_{15}$ according to their relative stabilities (Table 1), namely, S_1 is the most stable while S_{15} is the least stable. To our knowledge, the 15 structures reported here constitute the largest structural variety for the conformational space of the $^1Au_{10}$ system to date; this structural diversity, unnoticed in previous reports, is a consequence of the stochastic exploration of the PES [23–25]. Binding and relative energies together with relevant calculated quantities and the topological complexity of the structures are listed in Table 1.

One very important observation is that the global minimum on the $^1Au_{10}$ MP2/SDDALL PES is a 3D structure. A very well defined general trend is that more stable structures exhibit higher degrees of topological complexity in the electron densities; this becomes evident in an almost direct relationship between the number of bond critical points and binding energy (local exceptions are S_9, S_{14}); local fluctuations aside, it is seen that S_1, the most stable structure has the largest number of critical points of any kind while S_{15}, the least stable structure has the smallest number of critical points. This trend only applies to MP2 calculated relative energies. A Gaussian-like distribution of the Au–Au distances centered around 2.75 Å is shown in Figure 2 (2.47 Å is the experimental bond length for the dimer [31]). Vertical ionization potentials and electron affinities for the $^1Au_{10}$ clusters reported here (Table 1) are in the same range as those reported by Choi and coworkers [17], who also analyze the difference between calculated and experimental values.

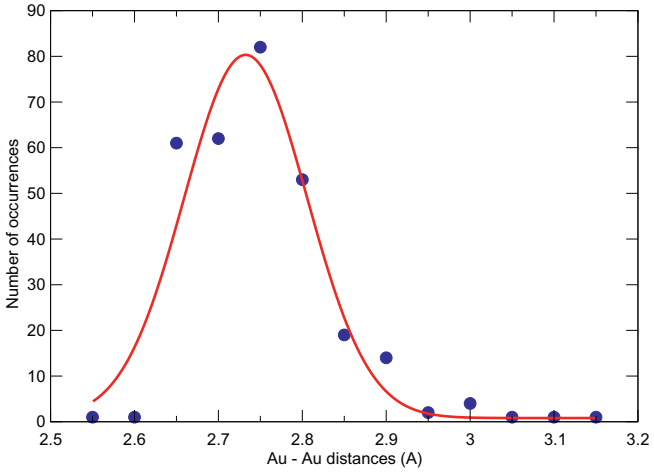

Figure 2. Radial distributions of the Au–Au distances in the MP2/SDDALL PES for the $^1Au_{10}$ clusters. The curve is centered around 2.75 Å; the equilibrium distance for Au_2 is 2.47 Å [31].

We relate the potential catalytic activity of the clusters to several molecular properties next. All LUMOs energies are negative, this gives the clusters elevated capacities to incorporate excess electrons, a very desirable property for catalysts involved in redox processes. The condensed Fukui function, $f^-(\mathbf{r})$, characterizes the sites of highest susceptibility for electrophilic attack on a given molecular system. Our calculations, performed along the lines proposed by Contreras and coworkers [32], predict the largest $f^-(\mathbf{r})$ values (up to 0.68) to be at the most peripheral, lowest coordinated Au atom in each cluster. Within QTAIM, $\lambda(A)$, the localization index gives the number of electrons that can be assigned to atom A [33–36]. In this work, the calculated localization indices also predict largest electron localizations in the most peripheral, lowest coordinated Au atom for each cluster. These two indicators suggest that more peripheral atoms have more available electrons to share with electron seeking molecules during the course of chemical processes. This result is in excellent agreement with previous reports of enhanced reactivity for peripheral Pt atoms in $^1Au_6Pt$ clusters [37].

3.3. Topological analysis of the electron densities

Bader's quantum theory of atoms in molecules (QTAIM) [38] has proven very successful in providing insights into bonding and other molecular properties. Critical points of the electron density

Table 1
Various relevant topological and energetical quantities for the $^1Au_{10}$ clusters calculated at the MP2/SDDALL level. BE: Binding energies (kcal/mol). ΔBE: Relative binding energies (kcal/mol). All energies are corrected for the unscaled ZPE energies. EA: Electron affinities (vertical, eV). IP: Ionization potentials (vertical, eV; experimental IP is 8.2 eV [43]). BCP, RCP, CCP denote the number of bond, ring and cage critical points respectively. $\sum_{BRC}$ gives the sum of the listed critical points. NDE is the total number of delocalized electrons for each cluster. All structures satisfy the Poincaré–Hopf theorem [38]. Structure notation is described in Fig. 1.

Structure	Symmetry	BE	ΔBE	EA	IP	BCP	RCP	CCP	$\sum_{BRC}$	NDE
S_1	D_{2d}	493.1	0.0	2.04	6.80	26	26	9	61	11.70
S_2	C_1	485.0	8.1	1.99	6.69	24	17	2	43	11.55
S_3	C_s	483.5	9.6	2.23	7.03	24	22	7	53	11.41
S_4	C_1	482.9	10.1	2.17	6.72	24	22	7	53	11.34
S_5	C_{2v}	481.3	11.8	2.15	6.92	22	16	3	41	11.13
S_6	C_s	477.5	15.6	2.13	6.79	19	12	2	33	10.55
S_7	D_{2h}	475.9	17.1	2.45	7.46	19	10	0	29	10.55
S_8	C_1	474.6	18.5	2.11	7.02	20	13	2	35	10.74
S_9	C_{3v}	471.9	21.2	1.01	6.92	24	20	5	49	11.42
S_{10}	C_{2v}	467.8	25.3	2.34	7.94	18	9	0	27	10.36
S_{11}	D_{2d}	464.0	29.1	1.56	7.65	18	10	1	29	10.17
S_{12}	C_2	451.4	41.6	2.27	7.96	15	6	0	21	9.74
S_{13}	C_s	448.0	45.1	1.79	7.32	16	8	1	25	9.85
S_{14}	D_{3h}	438.0	55.0	3.57	7.54	18	9	0	27	10.41
S_{15}	C_{2v}	436.9	56.1	2.47	7.27	15	6	0	21	9.67

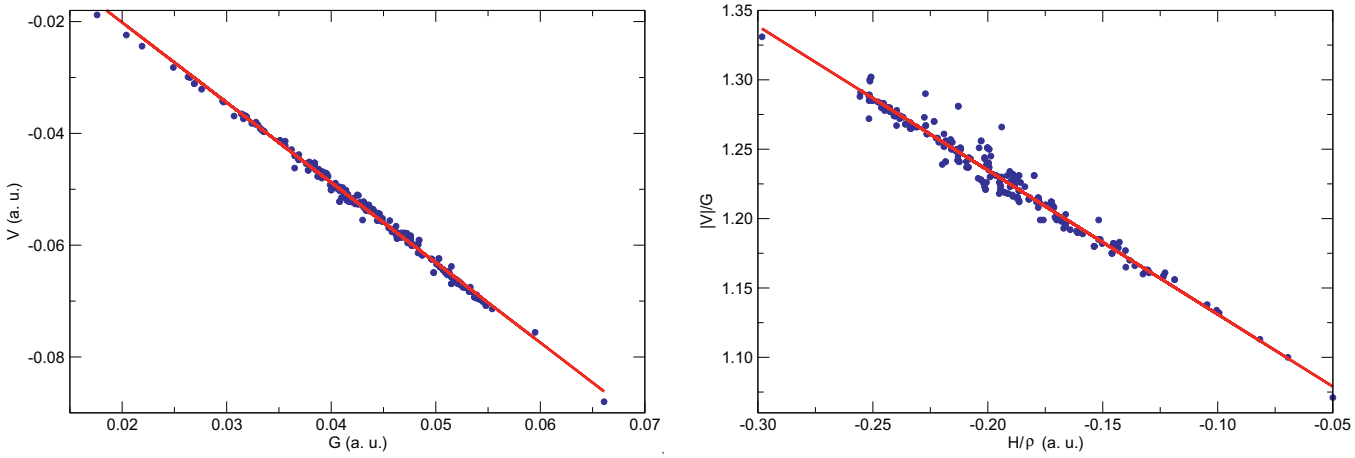

Figure 3. Left: relationship between the local kinetic and potential energy densities at all bond critical points in the MP2/SDDALL PES for the $^1Au_{10}$ clusters. Adjusted equation: $\mathcal{V}(\mathbf{r}_c) = -1.43\mathcal{G}(\mathbf{r}_c) + 0.01\, R^2 = 0.99$. Right: relationship between the $|\mathcal{V}(\mathbf{r}_c)|/\mathcal{G}(\mathbf{r}_c)$ ratio and the $\mathcal{H}(\mathbf{r}_c)/\rho(\mathbf{r}_c)$ ratio at all bond critical points in the MP2/SDDALL PES for the $^1Au_{10}$ clusters. $R^2 = 0.96$ for the adjusted line.

are those for which the gradient vanishes, $\nabla\rho(\mathbf{r}_c) = 0$. In this work, besides the above pointed out relationship between topological complexity of the electron density and cluster stability, we discuss bonding and bonding properties on the basis of several quantities evaluated at the bond critical points, specifically, the electron density $\rho(\mathbf{r}_c)$, its Laplacian $\nabla^2\rho(\mathbf{r}_c)$, the local electronic energy density $\mathcal{H}(\mathbf{r}_c)$, the local potential energy density $\mathcal{V}(\mathbf{r}_c)$ and the local kinetic energy density $\mathcal{G}(\mathbf{r}_c)$. Several criteria have evolved in the specialized literature to characterize bonding interactions, which within the QTAIM formalism, are thought to arise from closed shell (ionic, hydrogen bonding, etc.), shared (covalent), and intermediate interactions (contributions from both closed shell and shared interactions). We apply those ideas to characterize bonding in the $^1Au_{10}$ clusters.

The sign of the Laplacian of the electron density at a bond critical point is useful to characterize the dominating type of interactions: (i) for $\nabla^2\rho(\mathbf{r}_c) < 0$, the critical point is a local maximum in the electron density, meaning electrons are shared in the vicinities of $\mathbf{r}_c$ (ii) points for which $\nabla^2\rho(\mathbf{r}_c) > 0$ correspond to local minima in the electron density, resulting in electron density being concentrated away from the bond critical points, towards the nuclei, this is characteristic of closed shell interactions (iii) $\nabla^2\rho(\mathbf{r}_c) = 0$ marks the boundary between closed shell and shared interactions. In this work, Laplacians for all bond critical points are found to be positive, an early indication of non-shared interactions. On the other hand, some degree of covalency is expected because all energy densities at critical points are negative, $\mathcal{H}(\mathbf{r}_c) < 0$ [39], and because the largest $\rho(\mathbf{r}_c) \approx 0.073$, is smaller than 0.1, a well established cutoff for covalent interactions [40].

The local form of the virial theorem equates the Laplacian of the electron density to the potential and kinetic energy densities via $1/4\nabla^2\rho(\mathbf{r}_c) = \mathcal{V}(\mathbf{r}_c) + 2\mathcal{G}(\mathbf{r}_c)$ in atomic units [38]. Figure 3 (left) shows the relationship between the local potential and kinetic energy densities for all bond critical points in all $^1Au_{10}$ cluster conformations found in this work. A very well correlated linear trend is observed. This linear trend is in sharp contrast with the exponential relationships found in previous works for closed shell interactions in the form of several types of hydrogen bonds [41,42], indicating that interactions other than closed shell may play significant roles in bonding in Au clusters. The local form of the virial theorem leads to $\mathcal{V}(\mathbf{r}_c) = -2\mathcal{G}(\mathbf{r}_c)$ for vanishing Laplacians at the boundary of shared/non-shared interactions; in our case, Figure 3 (left) affords $\mathcal{V}(\mathbf{r}_c) \approx -1.43\mathcal{G}(\mathbf{r}_c) + 0.01$. The $|\mathcal{V}(\mathbf{r}_c)|/\mathcal{G}(\mathbf{r}_c)$ ratio was used by Espinosa and coworkers [39] to propose additional criteria

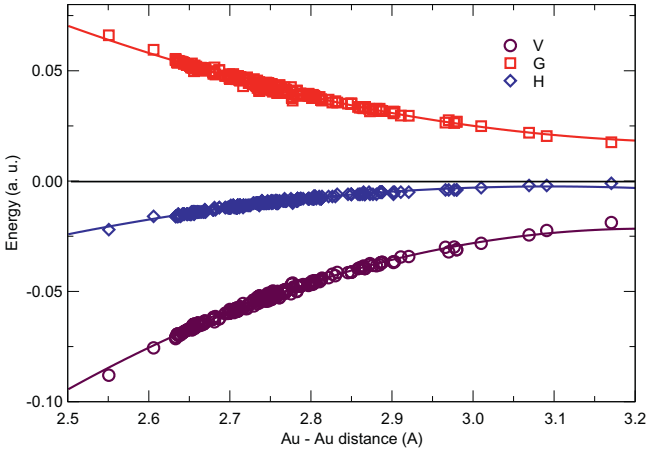

Figure 4. Local energy densities evaluated at all bond critical points as a function of the Au–Au distances in the MP2/SDDALL PES for the $^1Au_{10}$ clusters.

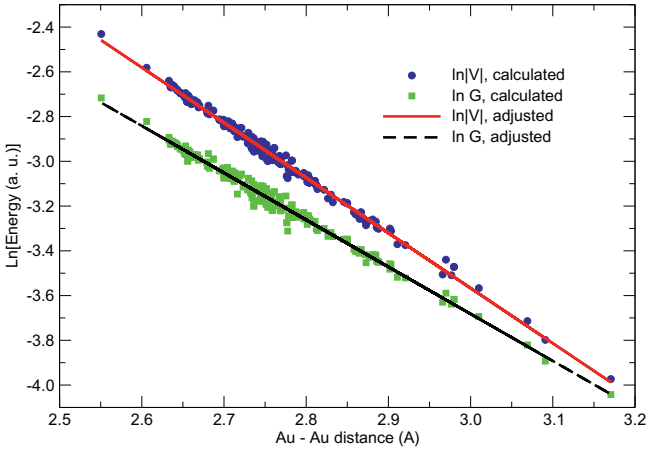

Figure 5. Local potential and kinetic energy densities evaluated at all bond critical points as a function of r, the Au–Au distances in the MP2/SDDALL PES for the $^1Au_{10}$ clusters. Adjusted equations: $\ln|\mathcal{V}(\mathbf{r}_c)| = -2.47r + 3.88, R^2 = 0.99$; $\ln|\mathcal{G}(\mathbf{r}_c)| = -2.10r + 2.62, R^2 = 0.99$.

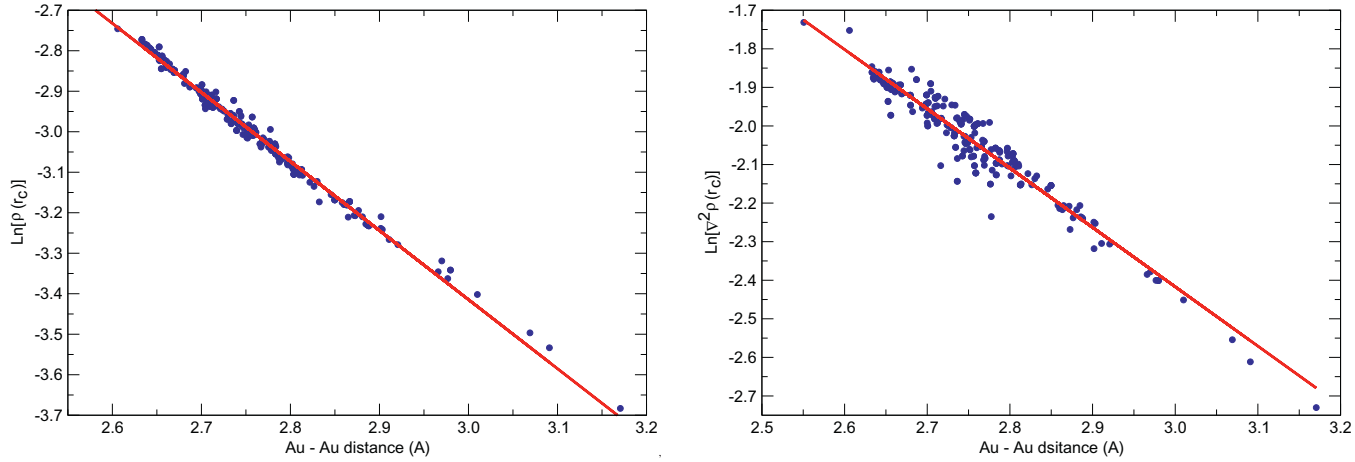

Figure 6. Logarithmic relationships for the $[r, \rho(\mathbf{r}_c)]$ (left) and $[r, \nabla^2\rho(\mathbf{r}_c)]$ (right) pairs, r being the Au–Au distances in the MP2/SDDALL PES for the $^1Au_{10}$ clusters. Adjusted equations: $\ln[\rho(\mathbf{r}_c)] = -1.7r + 1.7, R^2 = 0.99$ and $\ln[\nabla^2\rho(\mathbf{r}_c)] = -1.54r + 2.2, R^2 = 0.93$.

for the classification of interactions: ratios smaller than 1 correspond to closed shell interactions, ratios between 1 and 2 are deemed intermediate interactions while ratios larger than 2 are indicative of shared interactions. Figure 3 (right) shows the relationship between the $|\mathcal{V}(\mathbf{r}_c)|/\mathcal{G}(\mathbf{r}_c)$ ratio and $\mathcal{H}(\mathbf{r}_c)/\rho(\mathbf{r}_c)$, the bond degree parameter at all bond critical points for all $^1Au_{10}$ conformations. All ratios fall into the [1.07, 1.33] interval, an indicative of bonding intermediate between closed shell and shared interactions; the approximate decreasing linear trend means that larger ratios (more intermediate character) have both larger covalent (more negative $\mathcal{H}(\mathbf{r}_c)$) and larger non–covalent contributions.

The total electronic energy density at the critical points is given by $\mathcal{H}(\mathbf{r}_c) = \mathcal{G}(\mathbf{r}_c) + \mathcal{V}(\mathbf{r}_c)$. Figure 4 plots all local energy densities as a function of the Au–Au distances for all conformations. Figure 5 shows the dependency of $\mathcal{V}(\mathbf{r}_c), \mathcal{G}(\mathbf{r}_c)$ as a function of the separation between Au atoms. The first observation drawn from both plots, which is in excellent agreement with the information extracted from Figure 3 (right), is that at the BCPs, the energy contributions are largely dominated by the potential energy, which is negative (attractive) and larger in magnitude than the positive (repulsive) kinetic energy, the total energy being negative at all points. It is also seen that reducing the Au–Au distances results in the contributions from potential energy becoming more negative at a faster rate than the rate at which the kinetic energy becomes more positive; at larger distances the total energy approaches 0. We conclude that while all $\nabla^2\rho(\mathbf{r}_c) > 0$, characteristic of closed–shell interactions, the degree of electron sharing in Au–Au bonding increases for smaller Au–Au distances (larger $|\mathcal{V}(\mathbf{r}_c)|/\mathcal{G}(\mathbf{r}_c)$ ratios in the [1,2] interval and more negative $\mathcal{H}(\mathbf{r}_c)$ values). Further support for this interpretation is provided by Figure 6, where larger (shared) densities and Laplacians of the densities are predicted for smaller Au–Au distances.

The total number of delocalized electrons (*nde*) in a given cluster, we calculate as the difference between the total number of electrons (n) in the cluster and the sum the localization indexes for all atoms in the cluster: $nde = n - \sum_A \lambda(A)$. We found that the relative energy of the clusters is related to *nde* in a decreasing fashion (except for S_9 and s_{14}); we interpret this relationship as an additional covalency indicator in $^1Au_{10}$ bonding because as shown in Figure 7, the most stable clusters have more delocalized electrons and because as shown in the same figure, the electron density is larger at the bond critical points for clusters having larger *nde*, that is, the delocalized electrons (from the point of view of the atoms) accumulate in the bonding regions, making them more covalent. Finally, we also report that a perfect correlation (R^2 = 1.00) is observed between bond path lengths (BPLs) and Au–Au distances

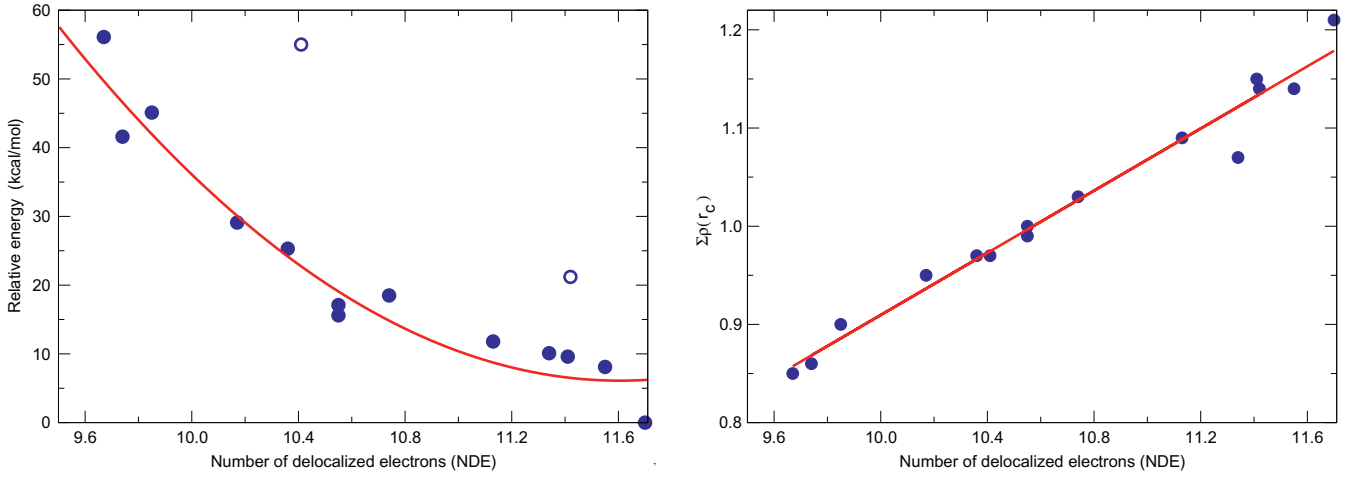

Figure 7. Relationships between the relative energy (left), total density at the bond critical points (right, $R^2 = 0.986$) with the total number of delocalized electrons for each cluster in the $^1Au_{10}$ MP2/SDDALL PES. Open circles correspond to S_9, S_{14}.

for all critical points in all $^1Au_{10}$ clusters, strongly indicating that bonding occurs along the straight lines directly connecting the atoms.

4. Summary and conclusions

We report a total of 15 stable conformations for $^1Au_{10}$. The isomers were obtained after random walks of the PM6 PES followed by analytical (gradient following) optimization of the candidate structures at the MP2/SDDALL level. Our global minimum is predicted to be a three dimensional structure belonging to the D_{2d} point group. Condensed Fukui functions and localization indices suggest that lowly coordinated, peripheral Au atoms have the potential to be more catalitically active sites in processes requiring the clusters to donate electrons. The topological complexities of the electron densities are directly related to cluster stability, with the most stable structure having the higher number of critical points of any kind. Despite all bond critical points having positive Laplacians, certain degree of covalency is expected in the clusters, bonding appears to be of intermediate character, with substantial contributions from both covalent and closed shell interactions. Several pieces of evidence support this claim, among them, the relationships between the total number of delocalized electrons (*nde*) with cluster relative energies and with the electron density at the bond critical points.

Acknowledgements

Partial funding for this work by Universidad EAFIT, internal project number 261-00002 is acknowledged. Financial support from Universidad de Antioquia, CODI office is also acknowledged.

Appendix A. Supplementary data

Supplementary data associated with this article can be found, in the online version, at http://dx.doi.org/10.1016/j.cplett.2012.04.030.

References

[1] M. Haruta, Catal. Today 36 (1997) 153.
[2] A. Templeton, W. Wuelfing, R. Murray, Acc. Chem. Res. 33 (2000) 27.
[3] R. Elghanian, J. Storhoff, R. Mucic, R. Letsinger, C. Mirkin, Science 277 (1997) 1078.
[4] P. Pyykkö, Chem. Soc. Rev. 37 (2008) 1967.
[5] H. Häkkinen, Chem. Soc. Rev. 37 (2008) 1847.
[6] P. Koskinen, H. Häkkinen, B. Huber, B. Issendorff, M. Moseler, Phys. Rev. Lett. 98 (2007) 015701.
[7] A. Herzing, C. Kiely, A. Carley, P. Landon, G. Hutchings, Science 321 (2008) 1331.
[8] M. Valden, X. Lai, D. Goodman, Science 281 (1998) 1647.
[9] J. Li, X. Li, H. Zhai, L. Wang, Science 299 (2003) 864.
[10] V. Bonačić-Koutecký, J. Burda, R. Mitric, M. Zampella, P. Fantucci, J. Chem. Phys. 117 (2002) 3120.
[11] J. Wang, G. Wang, J. Zhao, Phys. Rev. B 66 (2002) 035418.
[12] H. Häkkinen, U. Landman, Phys. Rev. B 62 (2000) 2287.
[13] A.J. Walker, Chem. Phys. 122 (2005) 094310.
[14] M. Sankaran, B. Viswanathan, Bull. Catal. Soc. India 5 (2006) 26.
[15] Y. Dong, M. Springborg, Eur. Phys. J. D 43 (2007) 15.
[16] B. Assadollahzadeh, P.J. Schwerdtfeger, Chem. Phys. 131 (2009) 064306.
[17] Y. Choi, W. Kim, H. Lee, K.J. Kim, Chem. Theory Comput. 5 (2009) 1216.
[18] X. Kuang, X. Wang, G. Liu, Eur. Phys. J. D 63 (2011) 111.
[19] X. Kuang, X. Wang, G.J. Liu, Mol. Model. 17 (2011) 2005.
[20] X. Kuang, X. Wang, G. Liu, Catal. Lett. 137 (2010) 247.
[21] X. Kuang, X. Wang, G. Liu, Eur. Phys. J. D 61 (2011) 71.
[22] L. Rincón, A. Hasmy, M. Marquez, C. Gonzalez, Chem. Phys. Lett. 503 (2011) 171.
[23] J. Pérez, A. Restrepo, ASCEC V-02: Annealing Simulado con Energía Cuántica. Property, development and implementation: Grupo de Química–Física Teórica, Instituto de Química, Universidad de Antioquia: Medellín, Colombia, 2008.
[24] J. Pérez, E. Flórez, C. Hadad, P. Fuentealba, A.J. Restrepo, Phys. Chem. A 112 (2008) 5749.
[25] J. Pérez, C. Hadad, A. Restrepo, Int. J. Quantum. Chem. 108 (2008) 1653.
[26] J.J. Steweart, Mol. Model. 13 (2007) 1173.
[27] D. Andrae, U. Haeussermann, M. Dolg, H. Stoll, H. Preuss, Theor. Chim. Acta 77 (1990) 123.
[28] J. Martin, A.J. Sundermann, Chem. Phys. 114 (2001) 3408.
[29] M.J. Frisch et al., Gaussian 09, Revision A.01, Gaussian, Inc., Wallingford CT, 2009.
[30] T. Keith, AIMALL (version 10.09.12), 2010 (aim.tkgristmill.com).
[31] G. Bishea, M.J. Morse, Chem. Phys. 95 (1999) 5646.
[32] R. Contreras, P. Fuentealba, M. Galván, P. Pérez, Chem. Phys. Lett. 304 (1999) 405.
[33] J. Poater, M. Sola, X.J. Fradera, Phys. Chem. A 105 (2001) 2052.
[34] J. Poater, M. Sola, M. Duran, X. Fradera, Theor. Chem. Acc. 107 (2002) 362.
[35] X. Fradera, M. Austen, R.J. Bader, Phys. Chem. A 103 (1999) 304.
[36] R. Bader, C. Matta, Inorg. Chem. 40 (2001) 5603.
[37] J. David, D. Guerra, C. Hadad, A.J. Restrepo, Phys. Chem. A 114 (2010) 10726.
[38] R. Bader, Atoms In Molecules: A Quantum Theory, Clarendon, Oxford, 1994.
[39] E. Espinosa, I. Alkorta, J. Elguero, E.J. Molins, Chem. Phys. 117 (2002) 5529.
[40] R. Bader, H.J. Essen, Chem. Phys. 80 (1984) 1943.
[41] E. Espinosa, E. Molins, Chem. Phys. Lett. 285 (1998) 170.
[42] O. Knop, K. Rankin, R.J. Boyd, Phys. Chem. A 107 (2003) 272.
[43] K. Taylor, C. Pettiette-Hall, O. Cheshnovski, R. Smalley, J. Chem. Phys. 96 (1992) 3319.